Aboveground Tree Biomass Density Mapping for Pilot Sites of Thimphu and Paro Dzongkhag, Bhutan Using NFI and ALOS PALSAR-2 mosaic data

དཔལ་ལྡན་འབྲུག་གཞུང་། སོ་ནམ་དང་ནགས་ཚལ་ལྷན་ཁག། ནགས་ཚལ་དང་གླིང་ག་ཞབས་ཏོག་ལས་ཁུངས།

Royal Government of Bhutan
Ministry of Agriculture and Forests
Department of Forests and Park Services

Aboveground Tree Biomass Density Mapping for Pilot Sites of Thimphu and Paro Dzongkhag, Bhutan Using NFI and ALOS PALSAR-2 mosaic data
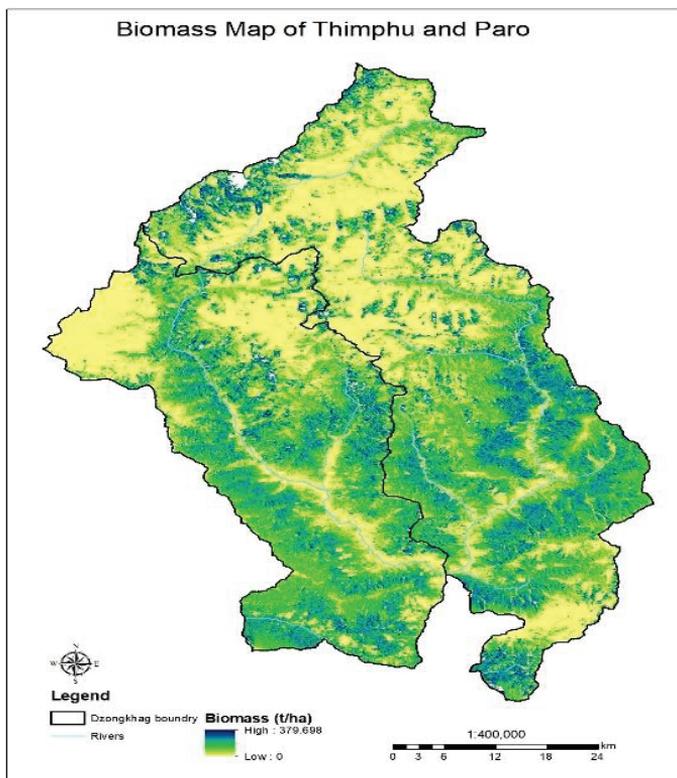

December 2018

Forest Resources Management Division

Department of Forest and Park Services

Report Prepared by:
1. Dorji Wangdi, Dy. Chief Forestry Officer, FRMD
2. Younten Phuntsho, Dy. Chief Forestry Officer, FRMD
3. Arun Rai, Dy. Chief Forestry Officer, FRMD
4. Dawa Zangpo, Sr. Forestry Officer

Report reviewed by:

1. Lobzang Dorji, Chief Forestry Officer, FRMD
2. Dr. Rajesh Bahadur Thapa, Capacity Building Specialist and SAR Expert, ICIMOD
3. Niroj Timalsina, Geospatial Solutions, ICIMOD

ACKNOWLEDGEMENT

Forest Resources Management Division.

Contents

Aboveground Tree Biomass Density Mapping for Pilot Sites of Thimphu and Paro Dzongkhag, Bhutan Using NFI and ALOS PALSAR-2 mosaic data

Background

Forest ecosystem play a vital role in carbon sequestration and carbon balance. Seventy one percent (FRMD, 2017; FRMD, 2016) country's geographical area is under forest cover which accounts for largest carbon sink in the country with total forest carbon stock of 709 million tonnes (FRMD 2018). The land use land cover maps of Bhutan (FRMD 2017) presents spatial coverage of forest cover but there is no spatial information on biomass and carbon stock of Bhutan. It is therefore necessary to accurately estimate the current distribution of forest carbon in aboveground biomass (AGB) for understanding of carbon dynamics and supporting national policies for climate change mitigation and adaptation.

Generally forest aboveground biomass is estimated through three available methods i) model based ii) measurement from traditional ground inventories , and iii) using remote sensing data set (as cited in Su et al, 2015). In this study, models were developed using the combination of forest inventory data and remote sensing data for mapping biomass for pilot sites in western Bhutan. A total of 149 NFI plots falling in the pilot sites were selected for developing models using ALOS-PALSAR-2 mosaic data of 2010 and 2015. Two biomass maps were generated from two best models- 1) simple model with one variable, and 2) complex model with multiple variables.

Data and method

Study Area

For this study two district namely, Paro and Thimphu Dzongkhag, located within the latitude of $27^0 07'28.93''$ N - $27^0 58'54.07''$ N and longitude of $89^0 08'08.22''$ E - $89047'38.44''$ E longitude in the western Bhutan, as depicted in the Figure 1was selected. The total area of Paro is 1,28,713 ha with 66282.67 ha (52%) Forest cover while that of Thimphu is 1,79,587 ha with 71213.78 ha (40%) under forest cover.
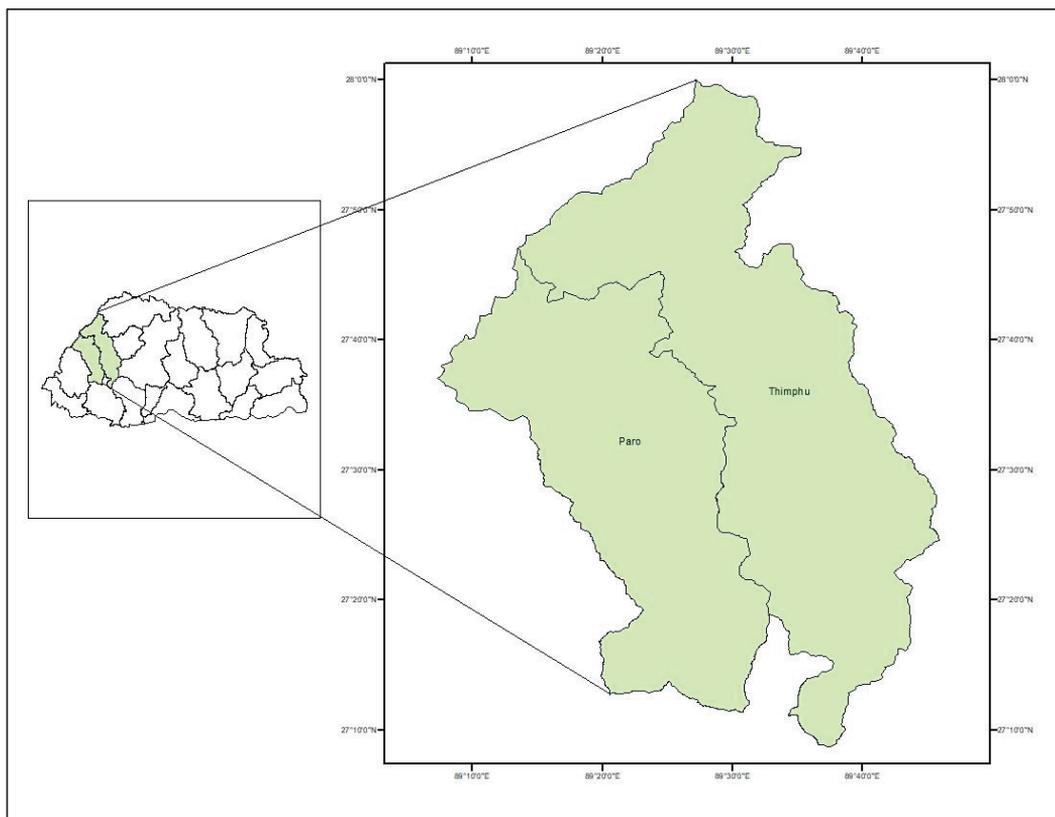
Figure 1: Study Area

Data

Ground Data

The biomass estimates generated at each NFI plot from NFI data were used as training data to develop model. For the pilot study, data from a total of 149 cluster plots falling within the study area were used ground data. The NFI plot consist of L-shaped cluster of plots spaced at 50m by 50 m apart. Each plot has radius of 12.62 m with 0.05 ha area Figure 2.

For the purpose of this study, new square plot of 0.57 ha (75.24 x 74.24 m) was generated using plot to plot distance (50 m) and plot radius (12.62 m) for all cluster plots. In this study, only aboveground tree biomass (AGTB) was estimated using 14 species specific and 2 general allometric equations and are converted into aboveground tree carbon (AGTC) using carbon fraction of 0.47 (IPCC, 2006).
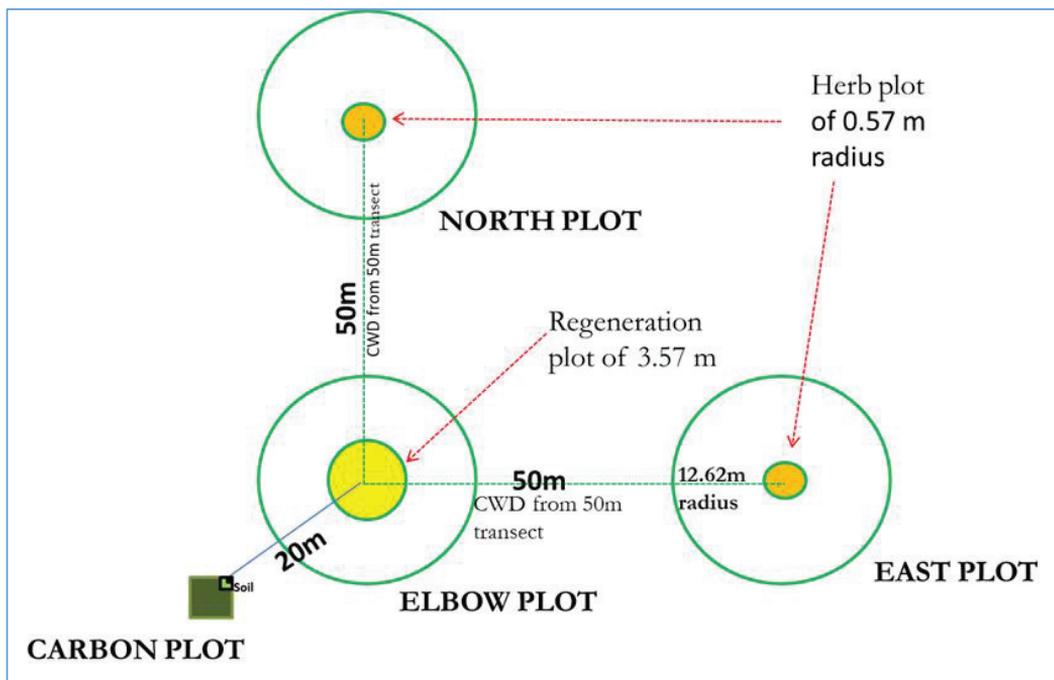
Figure 2: NFI sampling design (Source: NFI Field Manual, 2012)

The data from the pilot site - Paro and Thimphu, containing 149 sampling points were used for modeling. All the plots with zero biomass and inaccessible plots were ignored for the purpose of the modeling. The biomass density range from 0 to 400 tonnes per ha. On removing the zero and missing values, the total number of sampling plots were reduced to 92 sample plots. To detect the outlier the data (agb data), we have carried out outlier detection online using web based software graphpad software (https://www.graphpad.com/quickcalcs/Grubbs1.cfm) and Dixon's outlier test, Dixon's test for a single outlier, Grubbs' test for a single outlier, Rosner's Extreme Studentized Deviate test for multiple outliers (two sided test), Iglewicz and Hoaglin's robust test for (https://contchart.com/outliers.aspx.) These software did not detect any outliers in the ground measured data.

SAR Data Collection and Processing

Advanced Land Observing Satellite (ALOS) has consistently collected a large amount of data and provides wall to wall observation of earth surface at spatial resolution better than most Landsat imageries. Japanese Aerospace Exploration Agency (JAXA) has been providing free global 25m resolution PALSAR-2/PALSAR mosaic and forest/non-forest map for the year

2007, 2008, 2009, 2010, 2015, 2016 and 2017 (https://www.eorc.jaxa.jp/ALOS/en/palsar_fnf/data/index.htm).

The L-band data of ALOS/ PALSAR-2/PALSAR has the high sensitivity to forest structure and moisture content (Thapa, et al. 2015) and used for forest monitoring in Indonesia (Thapa, et al. 2015) and Tasmania, Australia (Lehmann, et al. 2012). The 25m resolution PALSAR-2/PALSAR imagery for study area was downloaded from JAXA website for the year 2010 and 2015 as field inventory was carried out between 2012 and 2015. We could not use the data for 2011, 2012, 2013 and 2014 as the similar mosaic were not available. The data comes in three formats of mask image, HH and HV channel images. The ALOS PALSAR-2/PALSAR mosaic product with spatial resolution of 25m in both HH and HV polarization for the year 2010 and 2015 was used. This also corresponds with our field data acquisition time (2012 to 2015). These data comes geometrically corrected (ortho-rectified) and topographically corrected (slope correction). However, we cannot rule out the presence of the some form of noise in the images and thus median filtering using 3 x 3 window was performed in ArcGIS 10.3 in for image enhancement (noise suppression).

The PALSAR-2 mosaic image with digital number (DN) are converted into gamma naught (γ^o) values in decibel unit (dB) using the following equation for each polarization forming the backscatter images.

$$\gamma^o = 10\, log_{10}\, (DN^2) + CF \qquad\qquad Equation\ 1$$

where, CF is a calibration factor and it is -83.0 dB for the PALSAR-2/PALSAR mosaic.

In addition to the backscatter images, we have created 5 ratio images following method described by Thapa et al. 2015.

$$R_{2010} = \frac{HV_{2010}}{HH_{2010}} \qquad\qquad Equation\ 2$$

$$R_{2015} = \frac{HV_{2015}}{HH_{2015}} \qquad\qquad Equation\ 3$$

$$R\,2D = \frac{HV_{2010} + HV_{2015}}{HH_{2010} + HH_{2015}} \qquad\qquad Equation\ 4$$

$$JR_1 = \frac{R_{2010\_2015}}{R_{2010}}$$ *Equation 5*

$$JR_2 = \frac{R_{2010\_2015}}{R_{2015}}$$ *Equation 6*

The ratio images were calculated using the dB values and not DN values. The dB values are converted into reflectance value using equation 7. We have generated four variables of reflectance for HH and HV channel for 2010 and 2015

$$Rf = 10^{(0.1*dB)}$$ *Equation 7*

We have also generated two Radar Forest Degradation Index (RFDI) is calculated using equation 8 for 2015 and 2010. Further, we created RFDI ratio image.

$$RFDI = \frac{HH_{Rf-}HV_{Rf}}{HH_{Rf+}HV_{Rf}}$$ *Equation 8*

Besides above created variable, we have generated another two mean variables for HV and HH channel using equation 9 and 10.

$$HV_{Mean} = \frac{HV_{2010} + HV_{2015}}{2}$$ *Equaiton 9*

$$HH_{Mean} = \frac{HH_{2010} + HH_{2015}}{2}$$ *Equaiton 10*

In total, we have generated 18 variables from ALOS PALSAR-2 images of 2015, 2010 and combined ratios of the two.

We used the mask image to identify and eliminate plots with no SAR backscatter information. The missing SAR backscatter information was by mask values of less than 255. The SAR backscatter values less than 255 are due to lack of data from land surface, backscatter information from water surface, layover and shadow effects as described in ALOS data products produced by Japanese Space Agency. There are also observation with zero biomass and NA for some plots of NFI. For the purpose of modeling, we have removed all plots with

zero and NA values as forested areas cannot have zero biomass while NA values were from inaccessible plots.

Model fitting

We used simple and multiple linear regression approaches to build relationship between SAR data (explanatory variable) and ground measured biomass estimate (response variable). We fitted simple linear regression models in Microsoft excel while multiple regression analysis was performed in SIGMA plot using step wise backward regression method. We used the p-value to identify the significance of the variable in the model. Indicators of regression including R^2 and P-value and model root mean square error (RMSE) were observed carefully. We have fitted 18 simple regression models and 14 multiple linear models.

Model 1: $\sqrt{ABTC} = \beta_0 + \beta_1(HH_{2015}) + \varepsilon$

Model 2: $\sqrt{ABTC} = \beta_0 + \beta_1(HV_{2015}) + \varepsilon$

Model 3: $\sqrt{ABTC} = \beta_0 + \beta_1(HH_{2010}) + \varepsilon$

Model 4: $\sqrt{ABTC} = \beta_0 + \beta_1(HV_{2010}) + \varepsilon$

Model 5: $\sqrt{ABTC} = \beta_0 + \beta_1(R_{2015}) + \varepsilon$

Model 6: $\sqrt{ABTC} = \beta_0 + \beta_1(R_{2010}) + \varepsilon$

Model 7: $\sqrt{ABTC} = \beta_0 + \beta_1(R_{2D}) + \varepsilon$

Model 8: $\sqrt{ABTC} = \beta_0 + \beta_1(JR_1) + \varepsilon$

Model 9: $\sqrt{ABTC} = \beta_0 + \beta_1(JR_2) + \varepsilon$

Model 10: $\sqrt{ABTC} = \beta_0 + \beta_1(RfHV_{2015}) + \varepsilon$

Model 11: $\sqrt{ABTC} = \beta_0 + \beta_1(RfHV_{2010}) + \varepsilon$

Model 12: $\sqrt{ABTC} = \beta_0 + \beta_1(RfHH_{2015}) + \varepsilon$

Model 13 $\sqrt{ABTC} = \beta_0 + \beta_1(RfHH_{2010}) + \varepsilon$

Model 14: $\sqrt{ABTC} = \beta_0 + \beta_1(RFDI_{2015}) + \varepsilon$

Model 15: $\sqrt{ABTC} = \beta_0 + \beta_1(RFDI_{2010}) + \varepsilon$

Model 16: $\sqrt{ABTC} = \beta_0 + \beta_1(RFDI_{ratio}) + \varepsilon$

Model 17: $\sqrt{ABTC} = \beta_0 + \beta_1(HV_{mean}) + \varepsilon$

Model 18: $\sqrt{ABTC} = \beta_0 + \beta_1(HH_{mean}) + \varepsilon$

Model 19: $\sqrt{ABTC} = \beta_0 + \beta_1(HH_{2015}) + \beta_2(HV_{2015}) + \beta_3(HH_{2010}) + \beta_4(HV_{2010}) + \beta_5(R_{2010}) + \beta_6(R_{2015}) + \beta_7(R2D) + \beta_8(JR_1) + \beta_9(JR_2) + \beta_{10}(RF\_HH_{2010}) + \beta_{11}(RF\_HV_{2010}) + \beta_{12}(RF\_HH_{2015}) + \beta_{13}(RF\_HV_{2015}) + \beta_{14}(RDDI_{2010}) + \beta_{15}(RDDI_{2015}) + \beta_{16}(RFDI\_ratio) + \beta_{17}(HH_{mean}) + \beta_{18}(HV_{mean}) + \varepsilon$

Model 20: $\sqrt{ABTC} = \beta_0 + \beta_1(HH_{2015}) + \beta_2(HV_{2015}) + \beta_3(HH_{2010}) + \beta_4(HV_{2010}) + \beta_5(R_{2010}) + \beta_6(R_{2015}) + \beta_7(R2D) + \beta_8(JR_1) + \beta_9(JR_2) + \beta_{10}(RF\_HH_{2010}) + \beta_{11}(RF\_HV_{2010}) + \beta_{12}(RF\_HH_{2015}) + \beta_{13}(RF\_HV_{2015}) + \beta_{14}(RDDI_{2010}) + \beta_{15}(RDDI_{2015}) + \beta_{16}(HH_{mean}) + \beta_{17}(HV_{mean}) + \varepsilon$

Model 21: $\sqrt{ABTC} = \beta_0 + \beta_1(HH_{2015}) + \beta_2(HV_{2015}) + \beta_3(HH_{2010}) + \beta_4(HV_{2010}) + \beta_5(R_{2010}) + \beta_6(R_{2015}) + \beta_7(R2D) + \beta_8(JR_1) + \beta_9(JR_2) + \beta_{10}(RF\_HH_{2010}) + \beta_{11}(RF\_HV_{2010}) + \beta_{12}(RF\_HH_{2015}) + \beta_{13}(RDDI_{2010}) + \beta_{14}(RDDI_{2015}) + \beta_{15}(HH_{mean}) + \beta_{16}(HV_{mean}) + \varepsilon$

Model 22: $\sqrt{ABTC} = \beta_0 + \beta_1(HH_{2015}) + \beta_2(HV_{2015}) + \beta_3(HH_{2010}) + \beta_4(HV_{2010}) + \beta_5(R_{2010}) + \beta_6(R_{2015}) + \beta_7(R2D) + \beta_8(JR_1) + \beta_9(JR_2) + \beta_{10}(RF\_HV_{2010}) + \beta_{11}(RF\_HH_{2015}) + \beta_{12}(RDDI_{2010}) + \beta_{13}(RDDI_{2015}) + \beta_{14}(HH_{mean}) + \beta_{15}(HV_{mean}) + \varepsilon$

Model 23: $\sqrt{ABTC} = \beta_0 + \beta_1(HH_{2015}) + \beta_2(HV_{2015}) + \beta_3(HH_{2010}) + \beta_4(R_{2010}) + \beta_5(R_{2015}) + \beta_6(R2D) + \beta_7(JR_1) + \beta_8(JR_2) + \beta_9(RF\_HV_{2010}) + \beta_{10}(RF\_HH_{2015}) + \beta_{11}(RDDI_{2010}) + \beta_{12}(RDDI_{2015}) + \beta_{13}(HH_{mean}) + \beta_{14}(HV_{mean}) + \varepsilon$

Model 24: $\sqrt{ABTC} = \beta_0 + \beta_1(HH_{2015}) + \beta_2(HV_{2015}) + \beta_3(HH_{2010}) + \beta_4(R_{2010}) + \beta_5(R_{2015}) + \beta_6(R2D) + \beta_7(JR_1) + \beta_8(JR_2) + \beta_9(RF\_HV_{2010}) + \beta_{10}(RF\_HH_{2015}) + \beta_{11}(RDDI_{2010}) + \beta_{12}(RDDI_{2015}) + \beta_{13}(HH_{mean}) + \varepsilon$

Model 25: $\sqrt{ABTC} = \beta_0 + \beta_1(HH_{2015}) + \beta_2(HV_{2015}) + \beta_3(HH_{2010}) + \beta_4(R_{2010}) + \beta_5(R_{2015}) + \beta_6(JR_1) + \beta_7(JR_2) + \beta_8(RF\_HV_{2010}) + \beta_9(RF\_HH_{2015}) + \beta_{10}(RDDI_{2010}) + \beta_{11}(RDDI_{2015}) + \beta_{12}(HH_{mean}) + \varepsilon$

Model 26: $ABTC = \beta_0 + \beta_1(HH_{2015}) + \beta_2(HV_{2015}) + \beta_3(HH_{2010}) + \beta_4(R_{2010}) + \beta_5(R_{2015}) + \beta_6(JR_1) + \beta_7(JR_2) + \beta_8(RF\_HH_{2015}) + \beta_9(RDDI_{2010}) + \beta_{10}(RDDI_{2015}) + \beta_{11}(HH_{mean}) + \varepsilon$

Model 27: $\sqrt{ABTC} = \beta_0 + \beta_1(HH_{2015}) + \beta_2(HV_{2015}) + \beta_3(HH_{2010}) + \beta_4(R_{2010}) + \beta_5(R_{2015}) + \beta_6(JR_1) + \beta_7(JR_2) + \beta_8(RF\_HH_{2015}) + \beta_9(RDDI_{2010}) + \beta_{10}(RDDI_{2015}) + \varepsilon$

Model 28: $\sqrt{ABTC} = \beta_0 + \beta_1(HV_{2015}) + \beta_2(HH_{2010}) + \beta_3(R_{2010}) + \beta_4(R_{2015}) + \beta_5(JR_1) + \beta_6(JR_2) + \beta_7(RF\_HH_{2015}) + \beta_8(RDDI_{2010}) + \beta_9(RDDI_{2015}) + \varepsilon$

Model 29: $\sqrt{ABTC} = \beta_0 + \beta_1(HV_{2015}) + \beta_2(HH_{2010}) + \beta_3(R_{2010}) + \beta_4(JR_1) + \beta_5(JR_2) + \beta_6(RF\_HH_{2015}) + \beta_7(RDDI_{2010}) + \beta_8(RDDI_{2015}) + \varepsilon$

Model 30: $\sqrt{ABTC} = \beta_0 + \beta_1(HV_{2015}) + \beta_2(R_{2010}) + \beta_3(JR_1) + \beta_4(JR_2) + \beta_5(RF\_HH_{2015}) + \beta_6(RDDI_{2010}) + \beta_7(RDDI_{2015}) + \varepsilon$

Model 31: $\sqrt{ABTC} = \beta_0 + \beta_1(HV_{2015}) + \beta_2(R_{2010}) + \beta_3(JR_1) + \beta_4(RF\_HH_{2015}) + \beta_5(RDDI_{2010}) + \beta_6(RDDI_{2015}) + \varepsilon$

Model 32: $\sqrt{ABTC} = \beta_0 + \beta_1(R_{2010}) + \beta_2(JR_1) + \beta_3(RF\_HH_{2015}) + \beta_4(RDDI_{2010}) + \beta_5(RDDI_{2015}) + \varepsilon$

Model Selection

The relationship between the independent variable such as backscatter coefficient and reflectance and dependent variable field measured aboveground biomass was build using regression approach (Thapa, et al. 2015). Step wise model calibration was performed for 32 models by comparing R^2 and RMSE. The trail version of Sigma plot was used for selection of significant variables. The backward stepwise regression analysis provides information the significant variables contributing to the models. The table 1 shows the coefficients, R^2, RMSE and Bias of regression models with single variable while table 2 shows R^2, RMSE, Bias and number of variables in multiple linear regression models.

$$RMSE = \sqrt{\frac{\sum_{i=1}^{n}(p_i - o_i)^2}{N}}$$

$$BIAS = \frac{\sum_{i=1}^{N}(p_i - o_i)}{N}$$

Table 1: Simple model coefficients, R square, RMSE and Bias

Model No.	β_0	β_1	R square	RMSE	Bias
Model 1	7.4532	0.5171	0.24	21.59	14.74
Model 2	9.453	0.457	0.29	15.767	3.064
Model 3	8.4597	0.7273	0.31	29.897	3.117
Model 4	10.454	0.5654	0.3663	27.457	2.863
Model 5	2.5324	0.6727	0.0074	42.97	4.480
Model 6	1.1022	1.4023	0.0341	41.821	4.36
Model 7	0.767	1.6313	0.0274	42.103	4.290
Model 8	6.1803	-2.5043	0.0091	42.903	4.473
Model 9	1.917	1.7787	0.004	43.121	4.496
Model 10	1.2878	37.878	0.2752	31.384	3.272
Model 11	0.4405	45.725	0.3607	27.679	2.886
Model 12	1.4541	10.878	0.1866	35.220	3.672
Model 13	0.4942	13.53	0.27	31.476	3.282
Model 14	8.4465	-8.706	0.1516	36.733	3.829
Model 15	8.8755	-9.4383	0.1385	39.010	4.067
Model 16	4.6492	0.9121	0.006	20.569	12.472
Model 17	10.602	0.5655	0.3844	14.082	2.776
Model 18	8.4703	0.6978	0.3106	14.712	3.11

Table 2: Multiple linear model R square, RMSE, Bias and Number of variables

Model No.	R^2	RMSE	BIAS	No. of variable
Model 19				18
Model 20	0.541	12.87	2.087	17
Model 21	0.439	12.85	2.05	16
Model 22	0.537	12.88	2.099	15
Model 23	0.536	12.913	2.188	14

Model 24	0.534	12.925	2.121	13
Model 25	0.531	12.943	2.139	12
Model 26	0.526	12.944	2.132	11
Model 27	0.505	12.850	1.665	10
Model 28	0.449	13.077	2.219	9
Model 29	0.484	13.359	2.287	8
Model 30	0.479	13.377	2.370	7
Model 31	0.457	13.43	2.345	6

Result

Based on the Table 1 and 2, we have selected one model each from simple linear regression approach and another from multiple linear regression approach. The equations for two selected models are described below while unselected model from simple linear regression can be obtained using the coefficients given in Table 1 while equations for unselected multiple linear model are described in appendix I.

Simple regression model

On the basis of R^2, RMSE and Bias, we have selected model 17 as the best fit model from simple linear regression for 18 predictor variables. It has highest R^2 and, lowest RMSE and Bias. The model equation is given below.

Model 17: ABTC = $(10.602 + 0.5655HV_{mean})^2$
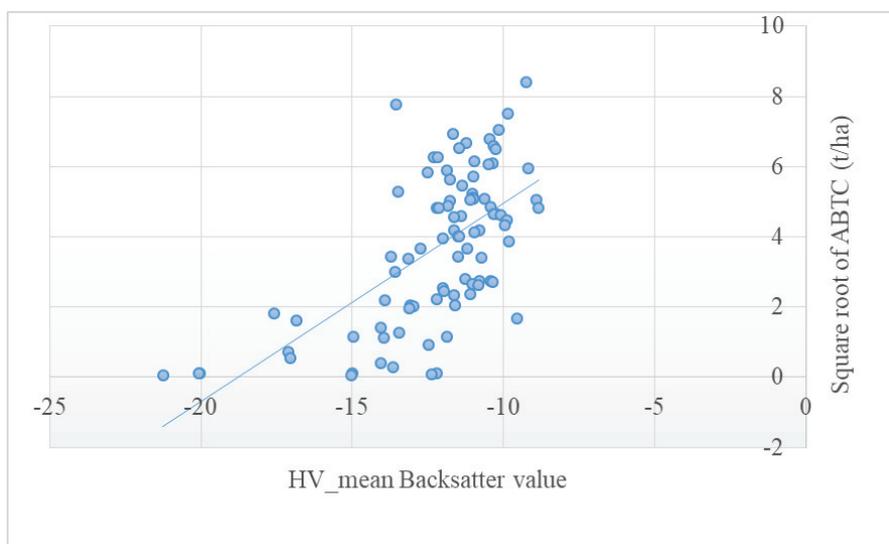
HV_mean Backsatter value
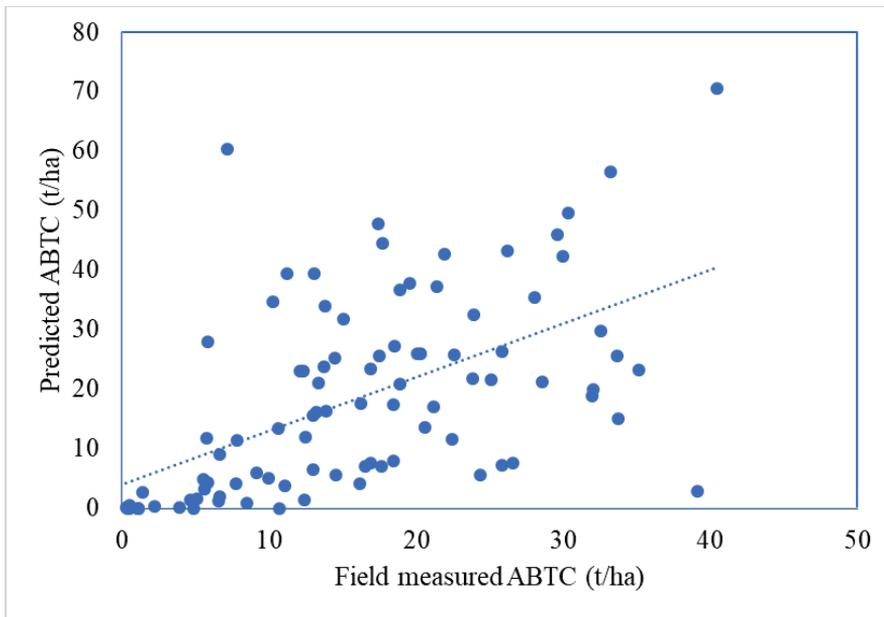
Figure 4: Comparison field measured and predicted ABTC of model 17

Multiple regression model

On the basis of R^2, RMSE and Bias, we have selected model 32 was selected as the best fit model from multiple linear regression for combination of different sets of 18 predictor variables. We have also taken into consideration that with every increase variable, the complexities of the model increases and we are also introducing some form of error. Although, the some models with more number of variable are performing better than the selected model in the form of RMSE and Bias, we wanted to keep the model simple while also performing as good as other models. The equation of the model is given below

Model 30: ABTC = (67.011+0.485* HV_2015_dB-11.263* R2010-54.606* JR1+33.109* Rf2015_HH-10.835* RFDI2010+30.055* RFDI2015)^2
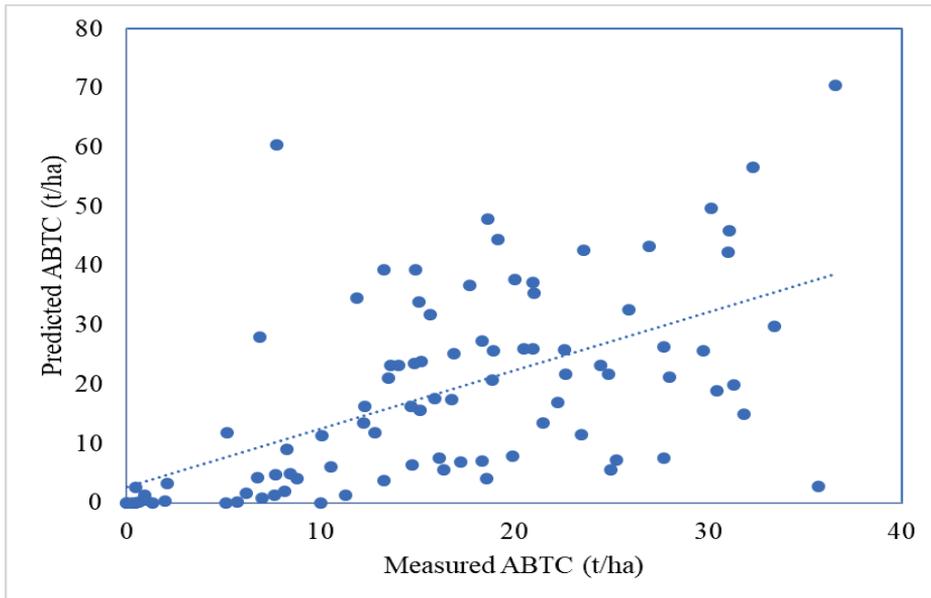
Figure 5: Comparison of field measured and predicted ABTC of Model 30

Development of maps

We have developed two biomass maps for model 17 and model 32. The map was developed with the help of Arc GIS 10.3 and QGIS 2.8.1. The figure 7 and 8 shows maps produced from model 17 and model 32 respectively. Since, the model are developed based on carbon, we have divided carbon density map with 0.47 to produce biomass map for both the models.
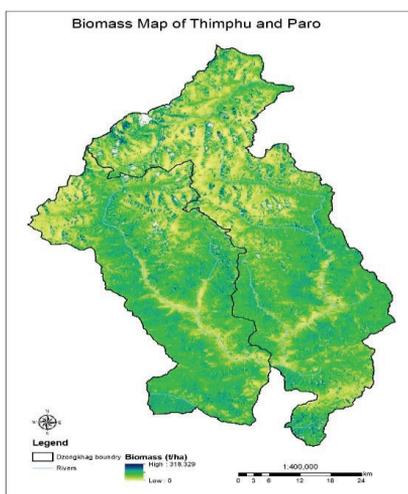

Figure 6: Biomass map of model 17
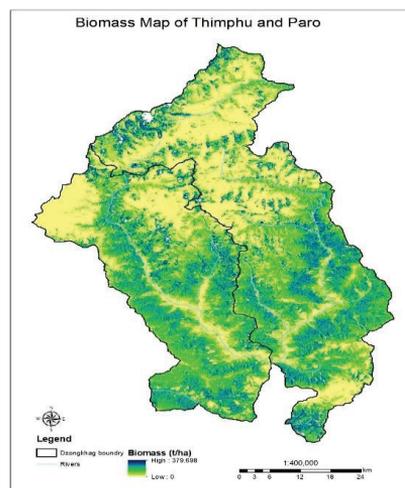
Figure 7: Biomass map of model 32

Limitations

This models have been developed using the MS Excel package and trial version of SIGMA plot. We have only used linear models and no attempts were made to model using other software packages. In many case, we can see the data is not normally distributed and are heteroscedastic. However, we did not model them. Moreover, the ground data is limited to tree above ground biomass/ carbon only while SAR data has an ability to detect the structure of entire land surface. Therefore, the models reported here warrants further verification and remodeling using appropriate software packages.

Conclusion

The ALOS PALSAR-2 mosaic has been used for biomass mapping in some tropical countries like Indonesia (Thapa et al.; 2015a, Thapa et al., 2015b; Thapa et al., 2015c), LiDAR data in Indonesia (Thapa et al.; 2015a) and San Francisco, USA (González-Jaramillo, et al., 2018), Du et al. (2014) used NFI and MODIS land cover product for mapping biomass in China and similar studies have been done in other parts of the globe. However, this is the first attempt to map Bhutan's biomass using remote sensing data in combination with ground measured NFI data. It observed that the SAR data of HV polarization is suitable for biomass modeling while ratios of HH and HV polarization of SAR data are poor predictor of biomass. The model using average SAR backscatter value of HV polarization has better predictability in comparison to other single variables.

It is evident that the multiple linear regression approach performs better than the simple linear regression. Therefore, it is desirable to explore other alternative method of linear modelling using other software packages.

Way forward

- Add the sapling
- Ecological zone wise modeling
- Improvement of the model : texture assessment of the radar image
- Increase the sampling plots
- Inclusion of the optical and texture in the improvement of the model
- Modeling for entire country.

References

FRMD. 2018. *National Forest Inventory Report Volume II*. Resources Management Division, Thimphu.

FRMD. 2017. *Land Use and Land Cover of Bhutan 2016. Map and Statistics*. Thimphu

FRMD. 2016. *National Forest Inventory Report Volume I*. Resources Management Division, Thimphu.

Kuntz, S. 2010. *Potential of Space borne SAR for Monitoring the Tropical Environments*. Tropical Ecology 51(1): p. 3-10.

Lehmann et al. 2012. *Forest Mapping and Monitoring In Tasmania Using Multi-Temporal Landsat and Alos-Palsar Data*. IGARSS 2012, Munich July 2012.

Mitchell, A.L., William, M. L. and Milne, A. K. 2011. *Forest and Forest Change Mapping using SAR data and a Robust Classification Methodology*. Proceedings of ACRS, Taiwan, Oct 3-7, 2011.

Thapa, et al. 2015. Calibration of Aboveground Forest Carbon Stock models for major tropical Forest in Central Sumatra Using Airborne LiDAR and Field Measurement Data." *IEE Journal of Selected Topics in applied earth observations and remote sensing* 661-673.

Thapa, R. B, T Motohka, M Watanabe, and M Shimada. 2015. "Time-Series maps of aboveground carbon stocks in th e forest of central Sumatra." *Carbon Balance and Management* 10-23.

Thapa, R. B., M. Watanable, T. Motohka, and M. Shimada. 2015. "Potential of high=resolution ALOS-Palsar mosaic texture for aboveground forest carbon tracking in tropical region." *Remote Sensing of Environment* 160: 122-133.

Appendix 1: Multiple linear regression models

Model 19: ABTC = (-61.321-9.891* HH_2015_dB+4.651* HV_2015_dB+2.863* HV_2010_dB-13.288* HH_2010_dB-41.984*R2010+19.344*R2015+15.526*R2D-104.758**JR1+159.989*JR2-51.754*Rf2010_HH+77.026*Rf2010HV+79.870*Rf2015_HH-41.222*Rf2015_HV-51.807*RFDI2010+108.235*RFDI2015+19.218*HH_avgmean-3.919*HV_avgmean)^2

Model 20: ABTC =(-67.065-10.567*HH_2015_dB+5.601*HV_2015_dB+2.784*HV_2010_dB-12.908*HH_2010_dB-40.350*R2010+22.037*R2015+14.304*R2D-97.381*JR1+154.319*JR2-45.138*Rf2010_HH+72.038*Rf2010_HV+52.079*Rf2015_HH-50.117*RFDI2010+116.242*RFDI2015+18.861*HH_avgmean-4.045*HV_avgmean)^2

Model 21: ABTC = (-54.903-9.709*HH_2015_dB+4.843*HV_2015_dB+1.591*HV_2010_dB-10.969*HH_2010_dB-34.668*R2010+12.854*R2015+12.651*R2D-65.017*JR1+114.386*JR2+29.083*Rf2010_HV+37.217*Rf2015_HH-38.556*RFDI2010+94.152*RFDI2015+16.870*HH_avgmean-3.095*HV_avgmean)^2

Model 22: ABTC = (-46.883-8.892*HH_2015_dB+4.204*HV_2015_dB-9.345*HH_2010_dB-35.515*R2010+15.007*R2015+11.484*R2D-71.230*JR1+112.884*JR2+32.603*Rf2010_HV+34.981*Rf2015_HH-44.036*RFDI2010+98.168*RFDI2015+14.624*HH_avgmean-1.014*HV_avgmean)^2

Model 23: ABTC = (-49.328-8.453*HH_2015_dB+3.552*HV_2015_dB-9.127*HH_2010_dB-31.287*R2010+12.076*R2015+10.030*R2D-57.966*JR1+101.190*JR2+42.177*Rf2010_HV+31.342*Rf2015_HH-29.157*RFDI2010+90.015*RFDI2015+13.667*HH_avgmean)^2

Model 24: ABTC = (-50.291-7.351*HH_2015_dB+3.599*HV_2015_dB-8*HH_2010_dB-30.553*R2010+18.514*R2015 -66.804*JR1+ 112.359*JR2 + 32.798*Rf2010_HV+ 41.687*Rf2015_HH-33.399*RFDI2010+98.234*RFDI2015+11.351*HH_avgmean)^2

Model 25: ABTC = (-26.243-6.200*HH_2015_dB+3.100*HV_2015_dB-7.705*HH_2010_dB-35.376*R2010+22.668*R2015 -95.252*JR1+120.469*JR2+53.159*Rf2015_HH-48.672*RFDI2010+103.113*RFDI2015+10.374*HH_avgmean)^2

Model 26: ABTC = (12.797-1.240*HH_2015_dB+2.595*HV_2015_dB-1.663*HH_2010_dB-28.600*R2010+16.625*R2015-

$$91.333*JR1+79.291*JR2+49.485*Rf2015\_HH-$$
$$38.037*RFDI2010+85.542*RFDI2015)^2$$

Model 27: ABTC = (20.438 +1.471*HV_2015_dB-1.718*HH_2010_dB-
28.410*R2010+15.983*R2015-
94.000*JR1+77.117*JR2+49.709*Rf2015_HH-
39.167*RFDI2010+72.481*RFDI2015)^2

Model 28: ABTC = (46.564 +0.654*HV_2015_dB-12.984*R2010-
53.269*JR1+17.809*JR2+40.716*Rf2015_HH-
16.667*RFDI2010+40.536*RFDI2015)^2

Model 29: ABTC = (53.091+0.481*HV_2015_dB-12.155*R2010-
50.150*JR1+9.592*JR2+35.958*Rf2015_HH-
11.999*RFDI2010+32.683*RFDI2015)^2

Model 30: ABTC = (67.011+0.485* HV_2015_dB-11.263* R2010-54.606* JR1+33.109*
Rf2015_HH-10.835* RFDI2010+30.055* RFDI2015)^2

Model 31: ABTC = (61.555-10.690* R2010-53.198* JR1+42.467* Rf2015_HH-12.252*
RFDI2010+22.155* RFDI2015)^2

ICIMOD

giz
Deutsche Gesellschaft
für Internationale
Zusammenarbeit (GIZ) GmbH

Federal Ministry for the
Environment, Nature Conservation
Building and Nuclear Safety